IEEE Photonics Journal
An IEEE Photonics Society Publication

Open Access

Photonic Generation of Binary Phase-Coded Microwave Signals With Large Frequency Tunability Using a Dual-Parallel Mach–Zehnder Modulator

Volume 5, Number 4, August 2013

Wei Li
Li Xian Wang
Ming Li, Member, IEEE
Hui Wang
Ning Hua Zhu, Member, IEEE

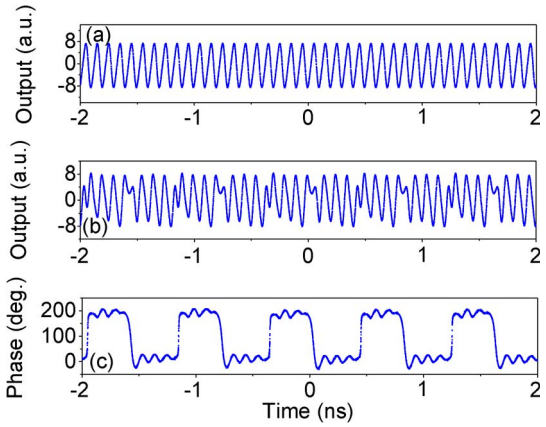

DOI: 10.1109/JPHOT.2013.2274771
1943-0655 ©2013 IEEE

IEEE photonics SOCIETY

IEEE

Photonic Generation of Binary Phase-Coded Microwave Signals With Large Frequency Tunability Using a Dual-Parallel Mach–Zehnder Modulator

Wei Li, Li Xian Wang, Ming Li, *Member, IEEE*, Hui Wang, and Ning Hua Zhu, *Member, IEEE*

State Key Laboratory on Integrated Optoelectronics, Institute of Semiconductors, Chinese Academy of Sciences, Beijing 100083, China

DOI: 10.1109/JPHOT.2013.2274771

Manuscript received June 28, 2013; revised July 18, 2013; accepted July 18, 2013. Date of current version August 6, 2013. This work was supported by the National Natural Science Foundation of China under Grants 61108002, 61127018, 61021003, 61177060, 61090390, 61275031, 61177080, and 60820106004. The work of M. Li was also supported by the "Thousand Young Talents" program. Corresponding author: N. H. Zhu (e-mail: nhzhu@semi.ac.cn).

Abstract: We present a photonic approach to generating binary phase-coded microwave signals with large frequency tunability using a dual-parallel Mach–Zehnder modulator (DPMZM). The DPMZM consists of a pair of sub-MZMs embedded in the two arms of a parent MZM. In our scheme, one of the sub-MZMs is fed by a sinusoidal microwave signal to be phase-coded, and the other sub-MZM is driven by a rectangular coding signal. The optical signals from the two sub-MZMs are destructively interfered by adjusting the dc bias of the parent MZM. As a result, the optical carrier is binary phase coded. A binary phase-coded microwave signal is generated by beating between the optical carrier and the sidebands. The carrier frequency of the phase-coded microwave signal is widely tunable. Phase-coded microwave signals with two different frequencies at 10 and 20 GHz are experimentally generated, respectively.

Index Terms: Microwave phase coding, microwave photonics, radar.

1. Introduction

In order to improve the range resolution of the radar systems, microwave pulse compression techniques have been widely utilized [1]–[3]. Phase coding or frequency chirping is generally introduced to the microwave pulses to increase the radar resolution via expanding the signal bandwidth and to transmit long pulses with a more efficient use of the average power. Phase-coded or frequency-chirped microwave signals have been generated using photonic technique. These methods are very attractive thanks to the large bandwidth provided by modern photonics devices and the low loss of the optical fiber. A lot of photonic-based techniques have been proposed to generate phase-coded or frequency-chirped microwave waveforms [4]–[14]. In [4] and [5], phase-coded or frequency chirped microwave pulses were generated utilizing a spatial light modulator (SLM). The system is very flexible since the SLM is easily reconfigurable. The main drawback of this approach is the complexity and high insertion loss due to the coupling between the optical fiber and space. All-fiber based methods are, therefore, more promising to generate phase-coded or frequency-chirped microwave signals [6]–[14]. It was reported that nonlinear frequency-to-time mapping were used to generate frequency-chirped microwave pulses [6]. Z. Li *et al.* and M. Li *et al.* have demonstrated the photonic generation of

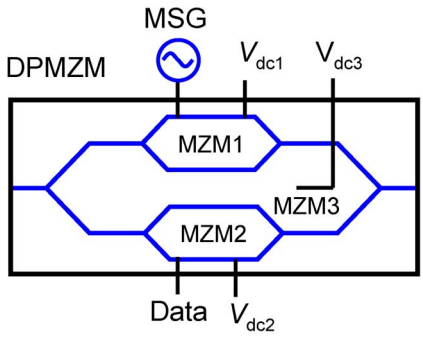

Fig. 1. Layout of the dual-parallel Mach-Zehnder modulator (DPMZM). MSG: microwave signal generator.

frequency-chirped and phase-coded microwave signals using a Sagnac interferometer and a Mach-Zehnder interferometer [7], [8], respectively. However, they suffer from the poor stability of the systems since the interferometers are very sensitive to the environmental fluctuation.

In [9], phase-coded microwave signals were generated using a polarization-maintaining (PM) fiber and a polarization modulator (PolM). The PM fiber was used to generate two orthogonally polarized optical signals. The frequency of the generated phase-coded microwave signal is not tunable for a given length of PMF. This problem was partly solved in [10], [11], where a PM-fiber Bragg grating (FBG) has been used. The PM-FBG enables frequency tunability in a limited frequency range because of its limited bandwidth. Phase-coded microwave signals were also generated based on PolMs and an optical bandpass filter [12], [13]. Again, the frequency tunable range is restricted by the optical filter. Recently, we have reported a microwave phase-coding technique using cascaded PolMs [14]. It should be noticed that the transmitters of these systems [6]–[14] are all realized using several individual components, which makes the transmitters complicated.

This paper presents a photonic binary phase-coded microwave signals generation technique with wide frequency tunable range using a single modulator. The modulator is actually a commercial dual-parallel Mach-Zehnder Modulator (DPMZM), which consists of a parent-MZM and two sub-MZMs. In our scheme, one of the sub-MZMs is driven by a microwave signal to be phase-coded and the other sub-MZM is fed by a rectangular data signal (i.e. coding signal). The optical carriers at the output of the sub-MZMs are destructively interfered via tuning the dc bias of the parent-MZM. By properly choosing the power of the electrical signal and the dc bias of the modulator, binary phase-coded microwave signals can be generated. We experimentally verified our approach at two microwave frequencies of 10-GHz and 20-GHz, respectively. The frequency tuning range of the proposed technique is determined by the bandwidth of the DPMZM.

2. Principle

Fig. 1 illustrates the layout of the DPMZM, which is structured as a parent-MZM (MZM3) and two sub-MZMs (MZM1 and MZM2). MZM1 and MZM2 are setting in parallel and are combined by MZM3. There are two high-speed radio-frequency (RF) electrodes integrated in the two sub-MZMs, respectively. The optical carrier can be expressed as $E_{\text{in}}(t) = E_0 \exp(j\omega_0 t)$, where E_0 and ω_0 are the amplitude and angular frequency of the optical carrier, respectively. A sinusoidal microwave signal is sent to MZM1. At the output of MZM1, the optical field is given by

$$\begin{aligned} E_{MZM1}(t) &= E_{in}(t)\cos(\beta_1 \cos\omega_m t + \varphi_1)/\sqrt{2} \\ &= E_{in}(t)\left\{\cos(\varphi_1)\left[J_0(\beta_1) + 2\sum_{n=1}^{\infty}(-1)^n J_{2n}(\beta_1)\cos(2n\omega_m t)\right]\right. \\ &\quad \left. + 2\sin(\varphi_1)\sum_{n=1}^{\infty}(-1)^n J_{2n-1}(\beta_1)\cos[(2n-1)\omega_m t]\right\}/\sqrt{2} \end{aligned} \quad (1)$$

where $\beta_1 = \pi V_m/(2V_\pi)$, and ω_m and V_m are the angular frequency and amplitude of the microwave signal, respectively. V_π is the half-wave voltage of the MZM1. $\varphi_1 = \pi V_{dc1}/(2V_\pi)$ and V_{dc1} is the dc bias voltage of MZM1. $J_n(\cdot)$ is the Bessel function of the first kind of order n. Under small-signal modulation condition, we only consider the first-order sidebands and (1) is rewritten as

$$E_{MZM1}(t) = E_0\{\cos(\varphi_1)\exp(j\omega_0 t) - \beta_1\sin(\varphi_1)\exp[j(\omega_0+\omega_m)t] - \beta_1\sin(\varphi_1)\exp[j(\omega_0-\omega_m)t]\}/\sqrt{2}. \quad (2)$$

On the other hand, a rectangular data signal is fed to MZM2. At the output of MZM2, we have the optical field

$$E_{MZM2}(t) = E_{in}(t)\cos[\beta_2 b(t) + \varphi_2]/\sqrt{2} \quad (3)$$

where $\beta_2 = \pi V_D/(2V_\pi)$, V_D is the amplitude of the rectangular data signal and $b(t) = 0$ or 1. $\varphi_2 = \pi V_{dc2}/(2V_\pi)$ and V_{dc2} is the dc bias voltage of MZM2. The outputs of MZM1 and MZM2 are combined by MZM3. Finally, we can write the output of DPMZM as

$$\begin{aligned} E_{DPMZM}(t) &= [E_{MZM1}(t) + E_{MZM2}(t)\exp(j\varphi_3)]/\sqrt{2} \\ &= \frac{1}{2}E_0\{\cos(\varphi_1) + \cos[\beta_2 b(t) + \varphi_2]\exp(j\varphi_3)\}\exp(j\omega_0 t) \\ &\quad - \frac{1}{2}E_0\beta_1\sin(\varphi_1)\exp[j(\omega_0+\omega_m)t] - \frac{1}{2}E_0\beta_1\sin(\varphi_1)\exp[j(\omega_0-\omega_m)t] \end{aligned} \quad (4)$$

where $\varphi_3 = \pi(V_{dc3} - V_{offset})/(2V_{\pi-MZM3})$ is the phase shift between the outputs of MZM1 and MZM2. It is tunable via adjusting the dc bias of the parent-MZM. $V_{\pi-MZM3}$ is the half-wave voltage of MZM3, V_{offset} is the offset voltage for $\varphi_3 = 0$. In our scheme, we bias MZM2 at its maximum transmission point, i.e. $V_{dc2} = 0$ V. The phase shift φ_3 is adjusted to be π by setting the dc bias of the MZM3. It means that the optical carriers at the outputs of MZM1 and MZM2 are destructively interfered. When the output signal of the DPMZM is detected in a photodetector (PD), the microwave signal is proportional to

$$i(t) = R|E_{DPMZM}(t)|^2 \propto -RE_0^2\{\cos(\varphi_1) - \cos[\beta_2 b(t)]\}\beta_1\sin(\varphi_1)\cos(\omega_m t) \quad (5)$$

where R is the responsivity of the PD. For $b(t) = 0$, the microwave current is given by

$$i_{m0}(t) = -RE_0^2[\cos(\varphi_1) - 1]\beta_1\sin(\varphi_1)\cos(\omega_m t). \quad (6)$$

For $b(t) = 1$, the current can be expressed as

$$i_{m1}(t) = -RE_0^2[\cos(\varphi_1) - \cos(\beta_2)]\beta_1\sin(\varphi_1)\cos(\omega_m t). \quad (7)$$

In order to generate a π phase-coded microwave signal, we have

$$\cos(\varphi_1) - \cos(\beta_2) = -[\cos(\varphi_1) - 1]. \quad (8)$$

It is worth noting that Eq. (8) is easy to be satisfied, e.g. $V_D = V_\pi$, and $V_{dc1} = 2V_\pi/3$. A schematic illustration of the principle of the proposed π phase-coded microwave signal generation technique is illustrated in Fig. 2. The output of MZM1 has three continuous wave (CW) signals, i.e. an optical carrier and two sidebands. For $b(t) = 0$ or 1, the amplitude of the optical carrier from MZM2 switches between 0 and twice of that from MZM1. As a result, the amplitude and phase of the sidebands keep constant and the phase of the optical carrier switches between 0 and π, while the amplitude of the optical carrier keeps unchanged. Binary phase-coded microwave signals are generated via beating between the optical carrier and the sidebands.

3. Experiments and Results

We carried out an experiment using the setup shown in Fig. 3. A laser diode (LD) emitting at 1550 nm served as the optical carrier. The output of the LD was coupled to a DPMZM via a PM fiber. A microwave signal generator (MSG) generated a sinusoidal microwave signal which was fed to MZM1,

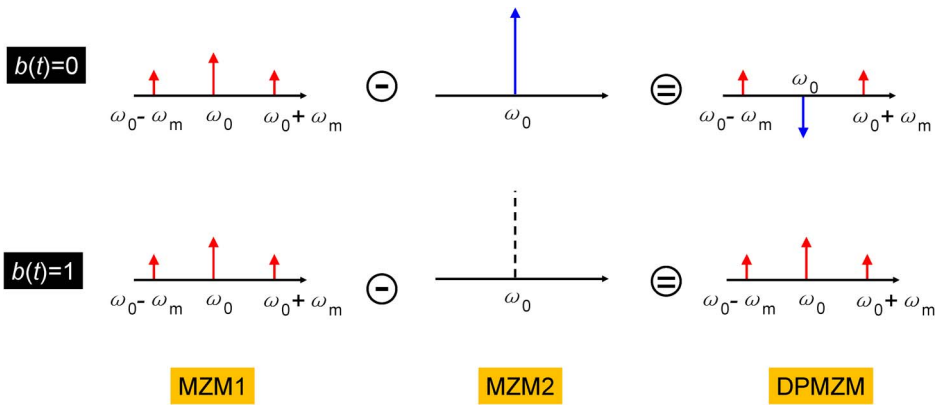

Fig. 2. Schematic illustration of the principle of the π phase-coded microwave signals generation technique.

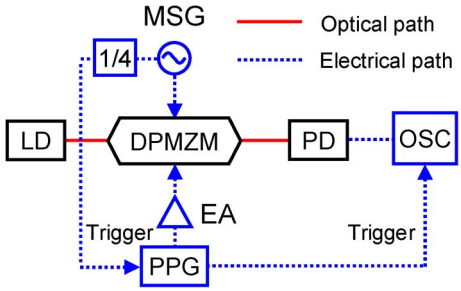

Fig. 3. Experimental setup of the proposed π phase-coded microwave signal generation system. LD: laser diode; DPMZM: dual-parallel Mach-Zehnder Modulator; MSG: microwave signal generator; EA: electrical amplifier; PPG: pulse pattern generator; PD: photodetector; OSC: oscilloscope.

while a rectangular data signal from a pulse pattern generator (PPG) was fed to MZM2. The PPG was triggered by the signal from the MSG after a 1/4 frequency divider. Therefore, the speed of the PPG as well as the speed of the phase-coded microwave signal is determined by the frequency of the microwave from the 1/4 frequency divider. The dc bias of the DPMZM and the power of the electrical signals were adjusted as described in section II. The phase-coded microwave signals were generated in the PD and were captured by a sampling oscilloscope (OSC).

First of all, we checked the phase-coding performance of the proposed system. The output frequency of the MSG was set at 10-GHz. The electrical data signal was a "0101" sequence of 2.5 Gb/s. Fig. 4(a) and (b) shows the non-coded and binary phase-coded 10-GHz microwave signal, respectively. We extracted the phase variation of the generated binary phase-coded 10-GHz signal, as shown in Fig. 4(c), using the Hilbert transform [15], [16] in MATLAB. It is apparent that the phase-shift is $\sim 180^\circ$ as predicted in the theoretical section.

The radar receiver operates the cross correlation between the microwave pulse and its echo to obtain a relatively narrow pulse. The pulse autocorrelation therefore plays an important role on the radar resolution. Next, we evaluated the pulse compression performance of the system. The data signal from the PPG was set as a 2.5 Gb/s pseudo-random bit sequence (PRBS) which has a length of 128 bits. The detection range of the practical radar system is expected to be extended using a longer PRBS pattern. The generated binary phase coded waveform is shown in Fig. 5(a), where the inset shows the zoom-in view. The autocorrelation of the generated signal is shown in Fig. 5(b). The zoom-in view shown in the inset exhibits a full width at half-maximum (FWHM) of $\sim$0.39 ns. The pulse compression ration (PCR) is defined as the ratio of the FWHM of the transmitted

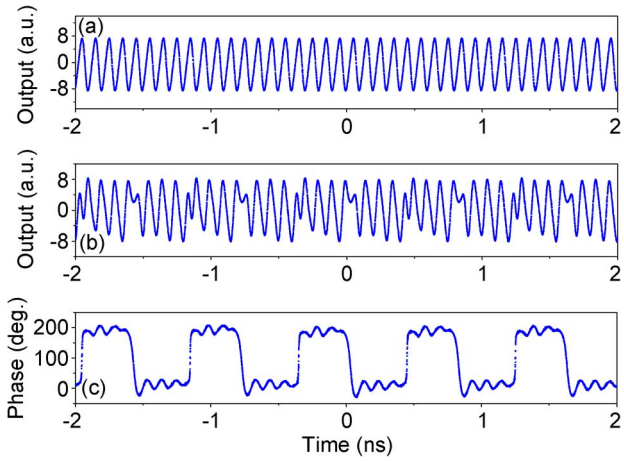

Fig. 4. (a) Generated non-coded 10-GHz microwave signal, (b) generated binary phase-coded 10-GHz signal, and (c) the phase-shift of the generated binary phase-coded signal.

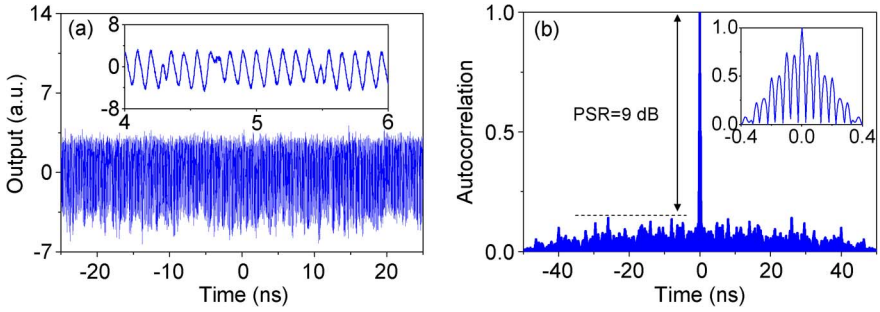

Fig. 5. (a) Generated 10-GHz binary phase-coded microwave signal and (b) the calculated autocorrelation of the signal with a PRBS phase-coding length of 128 bit at 2.5 Gb/s.

pulse to that of the compressed pulse, which is calculated to be ∼131. The peak-to-sidelobe ratio (PSR) is defined as the ratio of the peak power of the main lobe to that of the highest sidelobe, which is calculated to be 9 dB.

Finally, we evaluated the frequency tunability of the proposed system. To this end, the frequency of the MSG was set at 20-GHz. The electrical data signal from the PPG is a "0101" sequence at 5 Gb/s. Fig. 6(a) shows the non-coded microwave signal at 20-GHz. The binary phase-coded microwave signal at 20-GHz is shown in Fig. 6(b). The phase variation of the binary phase-coded 20-GHz signal was extracted using the Hilbert transform as shown in Fig. 6(c). Again, a π phase shifted microwave signal was achieved. We also evaluated the pulse compression performance of the system at the frequency of 20-GHz. The output of the PPG was a 5 Gb/s PRBS which has a length of 128 bits. Fig. 7(a) shows the generated 20-GHz phase-coded waveform and Fig. 7(b) illustrated its autocorrelation spectrum. The autocorrelation peak has a FWHM of about 0.2 ns. The PCR is ∼128 and the PSR is about 8.5 dB. The DPMZM used in our experiment is a commercially available device with a modulation bandwidth of ∼20-GHz for each sub-MZM. Therefore, we verified the proposed system up to a carrier frequency of 20-GHz. The stability of the system is expected to be significantly improved compared with the previous schemes using individual components since the DPMZM is an integrated device. Moreover, the dc biases of the DPMZM were controlled by a commercially available dc bias controller with self-feedback. The system steadily operated for several hours in our lab.

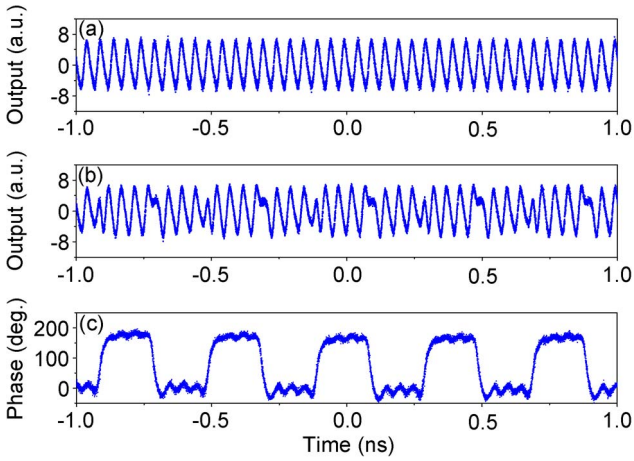

Fig. 6. (a) Generated non-coded 20-GHz microwave signal, (b) generated binary phase-coded 20-GHz signal, and (c) the phase-shift of the generated binary phase-coded signal.

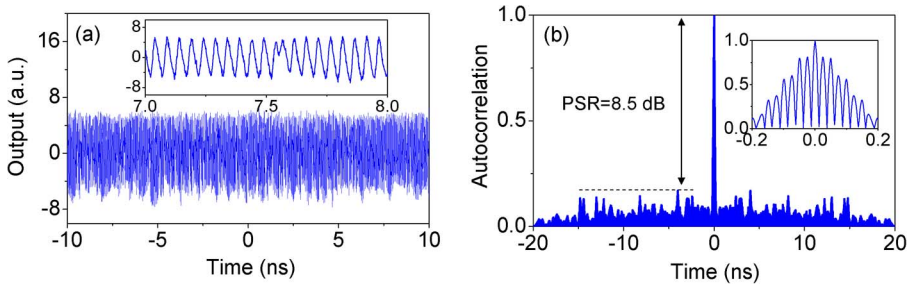

Fig. 7. (a) Generated 20-GHz phase-coded microwave signal and (b) the calculated autocorrelation of the signal with a PRBS phase-coding length of 128 bit at 5 Gb/s.

4. Conclusion and Discussion

A photonic approach to generating binary phase-coded microwave signals was proposed and experimentally verified using a DPMZM. The system complexity at the transmitter side was greatly reduced since only one integrated modulator was employed. The key feature of the proposed technique is that the carrier frequency of the phase-coded microwave signal is widely tunable. The generation of two phase-coded microwave signals at frequencies of 10-GHz and 20-GHz were experimentally demonstrated, respectively.

The proposed system was theoretically and experimentally demonstrated under small-signal modulation condition. For the microwave power beyond the small-signal modulation condition, the distortion of the system should be considered. In this case, the higher order modulation sidebands cannot be ignored. These higher-order sidebands will generate microwave signals corresponding to the harmonic of the original microwave signal. These harmonic signals are undesirable and have to be filtered out using a low-pass filter.

References

[1] M. I. Skolnik, *Introduction to Radar*. New York, NY, USA: McGraw-Hill, 1962.
[2] A. J. Seeds, "Microwave photonics," *IEEE Trans. Microw. Theory Tech.*, vol. 50, no. 3, pp. 877–887, Mar. 2002.
[3] M. Skolnik, "Role of radar in microwaves," *IEEE Trans. Microw. Theory Tech.*, vol. 50, no. 3, pp. 625–632, Mar. 2002.

[4] J. D. McKinney, D. E. Leaird, and A. M. Weiner, "Millimeter-wave arbitrary waveform generation with a direct space-to-time pulse shaper," *Opt. Lett.*, vol. 27, no. 15, pp. 1345–1347, Aug. 2002.
[5] J. Chou, Y. Han, and B. Jalali, "Adaptive RF-photonic arbitrary waveform generator," *IEEE Photon. Technol. Lett.*, vol. 15, no. 4, pp. 581–583, Apr. 2003.
[6] H. Chi and J. P. Yao, "All-fiber chirped microwave pulse generation based on spectral shaping and wavelength-to-time conversion," *IEEE Trans. Microw. Theory Tech.*, vol. 55, no. 9, pp. 1958–1963, Sep. 2007.
[7] Z. Li, W. Li, H. Chi, X. Zhang, and J. P. Yao, "Photonic generation of phase-coded microwave signal with large frequency tunability," *IEEE Photon. Technol. Lett.*, vol. 23, no. 11, pp. 712–714, Jun. 2011.
[8] M. Li and J. P. Yao, "Photonic generation of continuously tunable chirped microwave waveforms based on a temporal interferometer incorporating an optically-pumped linearly-chirped fiber Bragg grating," *IEEE Trans. Microw. Theory Tech.*, vol. 59, no. 12, pp. 3531–3537, Dec. 2011.
[9] H. Chi and J. P. Yao, "Photonic generation of phase-coded millimeter-wave signal using a polarization modulator," *IEEE Microw. Wireless Compon. Lett.*, vol. 18, no. 5, pp. 371–373, May 2008.
[10] Z. Li, M. Li, H. Chi, X. Zhang, and J. P. Yao, "Photonic generation of phase-coded millimeter-wave signal with large frequency tunability using a polarization-maintaining fiber Bragg grating," *IEEE Microw. Wireless Compon. Lett.*, vol. 21, no. 12, pp. 694–696, Dec. 2011.
[11] M. Li, Z. Li, and J. P. Yao, "Photonic generation of preciselyπ phase-shifted binary phase-coded microwave signal," *IEEE Photon. Technol. Lett.*, vol. 24, no. 22, pp. 2001–2004, Nov. 2012.
[12] Y. M. Zhang and S. L. Pan, "Generation of phase-coded microwave signals using a polarization-modulator-based photonic microwave phase shifter," *Opt. Lett.*, vol. 38, no. 5, pp. 766–768, Mar. 2013.
[13] L. X. Wang, W. Li, H. Wang, J. Y. Zheng, J. G. Liu, and N. H. Zhu, "Photonic generation of phase coded microwave pulses using cascaded polarization modulators," *IEEE Photon. Technol. Lett.*, vol. 25, no. 7, pp. 678–681, Apr. 2013.
[14] H. Wang, J. Zheng, L. Wang, J. Liu, L. Xie, and N. Zhu, "Photonic generation of chirp-free phase-coded microwave with accurate π phase shift and large continuous operating bandwidth," *IEEE Photon. J.*, vol. 5, no. 2, p. 5500306, Apr. 2013.
[15] S. L. Hahn, *Hilbert Transforms in Signal Processing.* Boston, MA, USA: Artech House, 1996.
[16] Z. Li, W. Li, H. Chi, X. Zhang, and J. P. Yao, "A continuously tunable microwave fractional Hilbert transformer based on a photonic microwave delay-line filter using a polarization modulator," *IEEE Photon. Technol. Lett.*, vol. 23, no. 22, pp. 1694–1699, Nov. 2011.